

# Chapter 2

## Predicting Materials' Performance

**Boris Ravdel**

**Abstract** One of the most vital challenges in lithium-ion battery engineering and manufacturing is related to the accurate prediction of cell's performance in various conditions (operating and storage temperature range, cycling rates, prolonged cycling, etc.). Macro-kinetic modeling of the processes occurring in the cell made tremendous progress during recent years. At the same time, substantial lack of data on intrinsic kinetic parameters, such as diffusion coefficients, exchange current, and their dependence upon lithium content in the solid materials restrains implementation of modeling. A practical approach to determining the proper form of the kinetic equations is presented in this chapter. This approach is based on interpretation of electrochemical measurements with respect to the structure of the electrode materials, and establishing the kinetic parameters, taking into account the connection between thermodynamic functions and kinetic parameters. The methodology refuses employing the concept of thermodynamic activity, but intensively uses empirical data of open circuit potentials (OCP) of the battery electrodes at varying degree of charge (DoC) measured at various temperatures. These data can also be useful for better understanding and prediction of most favorable voltage range for prolonged battery cycling life, and decrease the risk of catastrophic failures related to overtaxing the battery's active materials. Several examples of practical accomplishments of this approach are included in this chapter.

### 2.1 Editor's Note

For the reader, whose everyday "use" of electrochemistry is limited to the rather utilitarian consideration of simple formulas and approximated processes ongoing in the electrochemical cell (myself included), the following chapter may at first

---

B. Ravdel (✉)  
Yardney Technical Products, Inc., 2000 South County Trail, East Greenwich,  
RI 02818-1530, USA  
e-mail: bravdel@yardney.com

seem challenging. However, the included information is well worth the effort of brushing up on the principles and applications of fundamental electrochemistry.

Simply, the derivations presented here and in the related cited literature as well as the proposed experimental approach have direct use in speciality lithium-ion cells. The described analyses and their results have already assisted in fielded products with tens of thousands of delivered cycles (Fig. 2.1).

Another possible use of this material for the interested reader relates to the topic of lithium-ion cell modeling, which relies on similar foundations to the equations presented below, which are explicit despite being simplified. The simplification was done to convey the general concept; further reading is certainly encouraged.

## 2.2 Introduction: Macro and Intrinsic Kinetics

Generally, the electrochemical reaction is a heterogeneous, multi-step process. These steps can be consecutive or parallel; they can include homogeneous chemical reactions, transport processes, adsorption phenomena, crystals' nucleation and growing, as well as formation of new phases, etc. However, one essential step, always required to occur in the electrochemical reaction is the electron transfer through the electrolyte solution-electrode phase boundary. Thus, the electronic conductivity of at least one phase is crucial for the reaction to proceed. The overall reaction can involve several electrons; the electrons being transferred simultaneously or stepwise. In the latter case, other steps sometimes take place between the electron transfer steps.

### Text Box 2.1 Heterogeneous reactions [1]

*Heterogeneous reactions* constitute a class of chemical reactions where the reactants are components of two or more phases (solid and gas, solid and liquid, two immiscible liquids), or in which one or more reactants undergo chemical change at an interface, e.g., on the surface of a solid electrode.

An example of the simplest (in the sense of the number of kinetic parameters) electrochemical reaction is reduction of silver ions ( $\text{Ag}^+$ ) from a dilute aqueous solution of a well soluble silver salt (e.g., nitrate) in the presence of excess of an indifferent salt (e.g., potassium nitrate) on a liquid silver-mercury alloy (also called amalgam) electrode. Besides the transfer of a single electron, only diffusion steps are involved in this process. The entire reaction can be very well modeled and the kinetic parameters are determined experimentally with high level of accuracy. The information gleaned while analyzing the mechanism of silver ion reduction can be used in elucidating more complex, multi-step, multiphase processes, such as the electrochemical reaction in a lithium-ion cell.

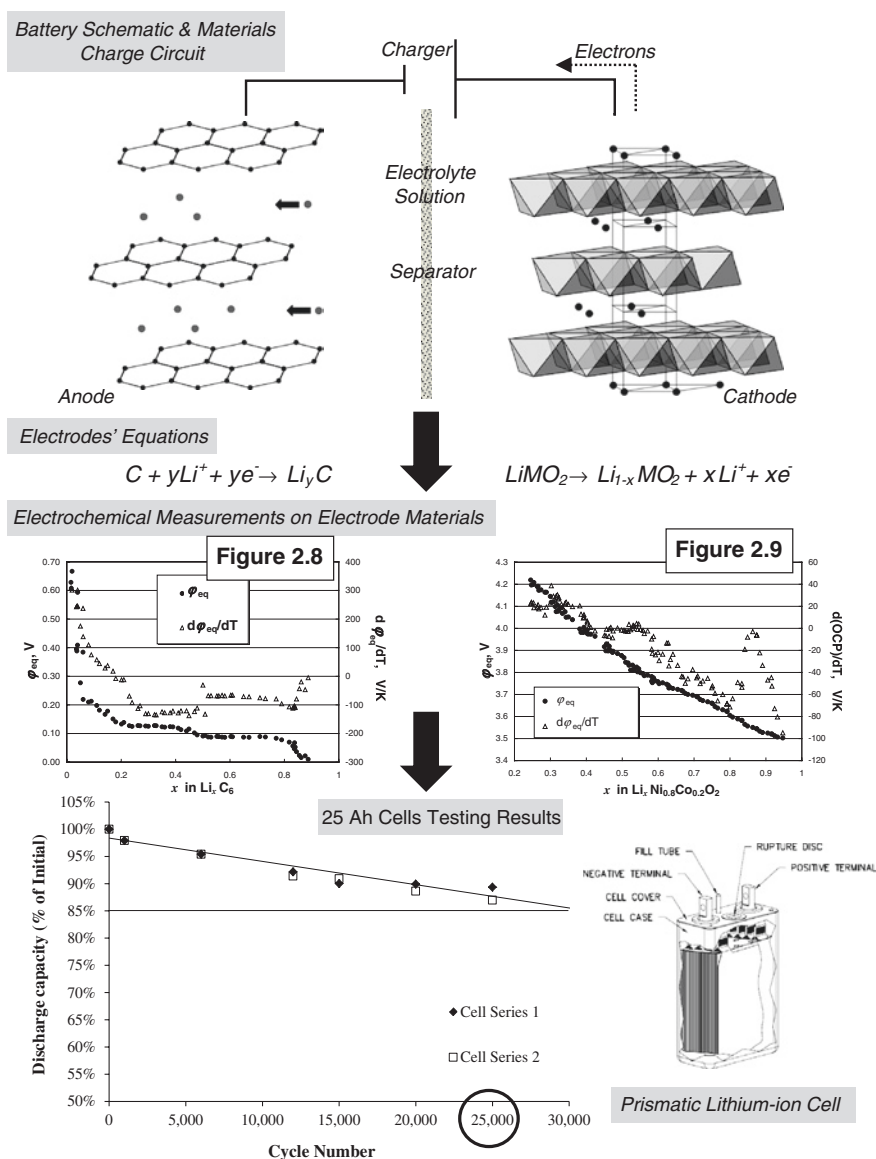


**Fig. 2.1** From fundamental properties of electrode materials to cell performance optimized for the fielded product

Active materials of lithium-ion electrodes<sup>1</sup> can be represented by the formula  $\text{Li}_x\text{Z}$  ( $0 < x < 1$ ). Here,  $x$  corresponds to that part of lithium content, which can reversibly leave the material (mobile lithium, in the form of  $\text{Li}^+$  ions). The moiety

<sup>1</sup> That is, the active materials of the electrodes employed in a lithium-ion cell.

Z may contain lithium and the stoichiometric indices in the explicit formula can be fractional (Text Box 2.2).

### **Text Box 2.2 Comments on selected moieties found within lithium-ion cathodes**

The term *moiety* in this text refers to the functional group of atoms found within the formula of electrode material. An example of the moiety Z (as in  $\text{Li}_x\text{Z}$ ) is the  $(\text{Li}_{0.45}\text{CoO}_2)$  group in the  $\text{Li}_{0.55}(\text{Li}_{0.45}\text{CoO}_2)$  notation of  $\text{LiCoO}_2$  formula. The notation gives information on the content of mobile lithium in the compound.

Many partially lithiated (i.e., when  $x < 1$ ) active materials in lithium-ion cells can be considered as solid solutions of mobile lithium (guest) in the host material—Z. Such host–guest material can be described by the similar set of thermodynamic equations as these used to characterize an amalgam. However, the mechanism of electrochemical reactions proceeding in a real cell is much more complex than in the case of the reaction of silver amalgam formation. There are many factors complicating the overall process:

- porous structure of the electrodes,
- low electron conductivity (as a rule) of the active material,
- presence of alien materials such as polymer binder and conductive diluents.

As the result, the basic electrochemical relationships binding the rate of the electrochemical reaction with the electrode potential are insufficient for the complete description of the cell processes. Instead, rather sophisticated macro-kinetic models have been developed. On the other hand, all models require quantitative data on several kinetic parameters. In the simplest case, it is enough to know the rate constant of the charge transfer step, or exchange current (EC), and diffusion coefficients (DC) in solid phase and electrolyte solution, assuming that both EC and DC depend on concentration.

Another term frequently used in modeling of electrochemical processes is polarization. Polarization, i.e., the shift of electrode potential from equilibrium state, is commonly employed as the driving force of electrochemical reaction. Consequently, the quantitative description of the discharging and charging processes in lithium-ion cell requires the knowledge of the equilibrium potential (EP) of electrodes as functions of degree of charge and temperature. In conventional electrochemistry, Nernst equation is used to determine the EP at given concentration and temperature. However, no general type of the dependence of EP on concentration and temperature is known or even suggested for lithium-ion electrode materials. Therefore, for all new cell chemistries (e.g., the active electrode materials described in Chap. 1) these relationships must be determined experimentally.

The overarching aim of the work described here was to establish a generalized description of the processes in lithium-ion cell that would apply regardless of

the exact chemistry of cell materials or nonequilibrium conditions. The approach taken in this publication relied on experimental observations, and the ultimate goal was the practical application. The application of this chapter would be the prediction of the complex electrochemical behavior of materials in an actual lithium-ion cell, based on the specific, easy to measure set of parameters.

In the course of this chapter, the simplest path of the overall process (diffusion, charge transfer, diffusion) is discussed, established by using phenomenological approach and focusing on the practical applications. Some conceptual challenges persist even at this simplified level, and are enumerated in the following text. The developed approach is applicable not only to the lithium-ion electrodes, but also to all electrochemically active solid phases (EASP).<sup>2</sup> In the following sections, the term EASP refers to a solid substance capable of electrochemical reduction or oxidation by species from another phase. Usually, the other phase is a liquid solution, but the participation of a second solid phase is possible. Oxidation or reduction processes involve changing the composition, as well as chemical and physical properties of EASP due to passing electricity through the EASP/solution boundary. It is important to note that the electrochemical and some accompanying chemical reactions in solid phase proceed at nonsteady-state conditions.

The interest in the analysis of the dependencies of equilibrium potential on composition of cathode materials for lithium-metal cells appeared in the late-1970s [2–8] where phase composition and phase transitions of oxides and halogenides of transient metals upon lithiation were discussed. The usefulness of the simultaneous scrutiny of the equilibrium potential together with its temperature coefficient was first proved in several works [9–13] published soon after. The approach to the calculation of kinetic parameters using the thermodynamic data, which is the subject of this chapter, has been proposed [14–16] later. In early 2000, new interest in the method has arisen, both in the thermodynamics of the processes within the electrodes for lithium-ion cells [17–22] and in the connection between thermodynamic functions and kinetic parameters [23]. In the series of recent works, M. Bazant [24] described the development of the fundamental theory of electrochemical kinetics and charge transfer applied to lithium iron phosphate (LFP).

## 2.3 Thermodynamics of Solid Electrodes

The knowledge of EP and the EP's dependence on electrode active material's composition at various temperatures is essential for calculations in the field of applied electrochemistry. Moreover, the EP ( $\varphi$ ) is directly proportional to the Gibbs energy ( $\Delta G$ ) for the electrochemical reaction, and EP's temperature

---

<sup>2</sup> The application of concepts discussed in this chapter can be extended onto alloy electrodes where insertion processes can occur, to electrochemical alloys' formation, etc.

coefficient (TCEP,  $d\phi/dT$ ) is proportional to entropy ( $\Delta S$ ) of the process. In other words, the EP and TCEP are Gibbs energy and entropy expressed in electrical units. Parallel scrutiny of both thermodynamic functions is a powerful tool of physicochemical analysis.

The concepts of EP and related open circuit potential and voltage (OCP and OCV), and electromotive force (emf) are well described in many textbooks on physical chemistry or electrochemistry. However, proving that the measured OCV (OCP) is indeed EP requires an approach that is specific to the particular electrochemical process being analyzed. For the EASP electrodes, a good confirmation of the  $\text{OCP} \equiv \text{EP}$  relationship is the stability of the OCV versus lithium-metal ( $\text{Li} \mid \text{Li}^+$ ) reference electrode over time and independence upon lithium ion's concentration. According to the IUPAC [25] rule, the electrochemical circuit for such measurements has the form



meaning that  $\text{Li} \mid \text{Li}^+$  is the reference electrode, at the potential of 0 V. As with other reference electrodes, when citing the OCV values measured versus  $\text{Li} \mid \text{Li}^+$ , the type of the reference electrode used in measurements should be stated because of the reference's impact on the measurements.

### 2.3.1 Ideal and Real Solutions

Bazant's theoretical work [24] exploits extensive knowledge of properties of LFP nanoparticles. LFP is a well-known and researched cathode material for lithium-ion batteries. The known characteristics of LFP include specifics of phase separation conditions, lithium-ion transport mechanism, elastic coherency strain, anisotropic nucleation and growth, interfacial energies, etc. Bazant's work and other similar approaches describing electrochemical processes in nonequilibrium conditions are crucial to the progress of applied electrochemistry in general and specifically, to forwarding developments in the field of intercalation materials-based batteries. The following section of this chapter compares the ideal and real systems, and the associated electrochemical solutions/equations.

If a reversible redox reaction:



proceeds on an electrode in the so-called "ideal solution", the dependence of the EP upon reactants' concentrations,  $[\text{Ox}]$  and  $[\text{Red}]$ , follows the Nernst equation:

$$\phi = \phi^\circ + \frac{RT}{nF} \ln \frac{[\text{Ox}]}{[\text{Red}]} \quad (2.3)$$

where  $\phi^\circ$  is the standard potential at standard values of the both reactants' concentrations, and  $R$ ,  $T$ , and  $F$  denote the universal gas constant, the absolute

temperature, and the Faraday constant, respectively. In fact, Eq. 2.3 is a transition of the formula for the chemical potential of ideal gas:

$$\mu = \mu^\circ + RT \ln P \quad (2.4)$$

$\mu^\circ$  is [26] the standard value of the chemical potential at standard pressure  $p^\circ$ , and the dimensionless value  $P = p/p^\circ$  is the ratio of the actual gas pressure over the standard pressure  $p^\circ$ . The real dependence of the EP upon concentration follows the Nernst relationship only at low concentrations (below  $0.001 \text{ mol L}^{-1}$  in aqueous solutions).

Similarly, Eq. 2.4 poorly describes the behavior of gases at pressure above 50 atmospheres. In order to retain the appearance of the ideal-gas thermodynamic equations, but render them applicable to real gases, an American chemist G.N. Lewis introduced the concept of fugacity in 1901 [27]. The ideal gas pressure  $p$  and fugacity  $f$  is related through the dimensionless fugacity coefficient  $g = f/p$ . The fugacity coefficient has clear physical meaning, and describes the deviation in behavior of a real gas compared to an ideal gas.

Indeed, all gases follow the general equation

$$\left( \frac{\partial \mu}{\partial p} \right)_T = \underline{v} \quad (2.5)$$

where  $\underline{v}$  is the gas molar volume. For an *ideal* gas, the equation of state has the form:

$$p\underline{v} = RT \quad (2.6)$$

For a *real* gas, other equations of state must be used, e.g., van der Waals, Berthelot, Diterichi, or Kammerling-Onnes [28]. Integration of Eq. 2.5 using Eq. 2.6 leads to the relationship shown in Eq. 2.4. In this case, standard chemical potential appears formally as the integration constant. Of course, integrating of Eq. 2.5 with a real gas equation of state will produce other forms of chemical potential equation than in the case of the ideal gas equation; the difference between the outcomes of integration uniquely defines the fugacity coefficient.

There is no single equation of state for the electrolyte solutions, but similarly to the concept of fugacity, the concept of thermodynamic activity is commonly engaged. The activity exhibits dependence on concentration.

By the IUPAC [25] definition, the activity ( $a$ ) is the anti-logarithm of the chemical potential and does not constitute a new physical entity:

$$a = \exp \left( \frac{\mu - \mu^\circ}{RT} \right) \quad (2.7)$$

The concept of activity (Eq. 2.7) merely puts into operation *another function of chemical potential* and converts the chemical potential into a form that is convenient for calculations. Specifically, the thermodynamic functions can be calculated using the formulae derived for ideal gases by substitution of the pressure with the activity. In other words, the form of the definition (Eq. 2.7) is dictated by the

wish to keep the formal similarity between the expressions for chemical potentials of ideal gas and a solution component. The activity is reciprocally bound with the standard value of the chemical potential. Since the standard chemical potential is equal to the chemical potential of the species in the *hypothetic* solution in which both activity and activity coefficient are equal to 1, the direct measurement is therefore impossible. Both standard potentials and activities (activity coefficients) must be calculated using one of several available modeling approaches. Computational procedures are not simple, and some problems are essentially irresolvable (e.g., the problem of the activity coefficient of a single ion; instead the *mean ion activity coefficient* is used). Nevertheless, the values of activity coefficients have been determined for many ions in various aqueous solutions. However, the collection of activity coefficients for ions in nonaqueous solutions is much scarcer.

The above-mentioned considerations pertained to computational challenges with analyzing electrochemical processes involving real gases and solutions. New set of difficulties arises with attempts of determining the activities (or activity coefficients) for solid phases comprised of multiple components. For example, the *empirical* Raoult and Henry laws that bind the concentrations of the solutions' components to their vapor pressures can hardly be practically applied for solids. Similarly, van't Hoff's law of osmotic pressure that formally implies the equation of state of ideal gas to the solution [28] is not applicable to solids. Indeed, the pressure of the solid solution (e.g., metal alloy) components is usually immeasurable within wide temperature range, and osmotic pressure is not detected in solids. This aspect is very prominent in EASP where lithium is dispersed in the host matrix.

Last but not the least problem with unified approach to electrochemical processes across various states of matter is the use of molar fraction [25] as the unit of concentration in electrochemical equations. Such choice of the concentration unit implies that the EP would exhibit *a very simple dependence* on the presence of the so-called indifferent electrolyte. By this logic, the potential of  $\text{Ag} \mid \text{Ag}^+$  electrode in aqueous solution (e.g.,  $0.1 \text{ mol L}^{-1}$  of silver nitrate) should depend on the addition of sodium nitrate since the molar fraction of silver ions is changed by the addition of the indifferent salt ( $\text{KNO}_3$ ) even if the molar-volumetric concentration of  $\text{Ag}^+$  ions remains constant. Moreover, the substitution of sodium salt with any other apparently indifferent salt (potassium, ammonium, alkyl-ammonium salt, etc.) is expected to shift the EP to new values. However, the indifferent (or supporting) electrolyte in common electrochemical practice is considered to be only affecting (stabilizing) the activity coefficient. On the other hand, the unanswered question persists whether the potentials of *ideal* silver-mercury and silver-gold alloy electrodes in silver nitrate solution are *equal* when silver *mole fractions* are *equal*, or when the silver *molar-volumetric concentrations* are *equal*.

The above-mentioned issues also pertain to the selection of the standard state of EASP. As a matter of fact, on  $\text{Li}_x\text{Z} \mid \text{Li}^+$  electrode, either at  $x = 0$  or at  $x = 1$ , no equilibrium conditions corresponding to lithium exchange can be established. The reasoning presented earlier illustrates that the application of the concept of thermodynamic activity to the EASP is impractical and may not be attainable.



### 2.3.2 Equilibrium Potentials on EASP

In order to define an alternative approach to employment of thermodynamic activity, a few basic assumptions must be established. First, let the oxidation or reduction reaction of EASP proceed with participation of a univalent cation from the electrolyte (e.g.,  $\text{Li}^+$ ). In reaction:



$\text{Li}_x\text{Z}$  and  $\text{Z}$  are reduced and oxidized forms of EASP, while  $x \leq 1$ . The symbol “ $\rightleftharpoons$ ” indicates that the reaction can proceed in both directions. However, in order to achieve the potential-determining reaction, it is more convenient to rewrite Eq. 2.8 so that the  $\text{Li}^+$  coefficient equals 1. The modified equation is



Obviously, the EP can establish only on partially discharged electrode, that is, at  $1 < p < 0$  (or  $0 < x < 1$ ), but the fact that steady state OCV (OCP) is equal to the true EP remains yet to be proven.

Modifying the proposed EP-determining reaction on the  $\text{LiZ}_p \mid \text{Li}^+$  electrode so that Eq. 2.9 is achieved clarifies the fact that the character of dependence of the electrode's EP upon lithium ions' concentration in the solution is the same as that of  $\text{Li}(\text{metal}) \mid \text{Li}^+$  electrode (Eq. 2.9).<sup>3</sup>

$$\frac{\partial \phi_{\text{EASP}}}{\partial [\text{Li}^+]} = \frac{\partial \phi_{\text{Li}(\text{metal})}}{\partial [\text{Li}^+]} \quad (2.10)$$

Moreover, the equality of EP dependence on  $\text{Li}^+$  concentration in solution with the  $\text{Li} \mid \text{Li}^+$  metal electrode relationship is regardless of the application of the Nernst's law and the units in which lithium ion concentration in the solution is expressed. Thus, if the experimental measurements confirm the independence of the cell's OCV (Eq. 2.11) upon lithium ion concentration in the solution, the potential on the EASP can be treated as EP.



### 2.3.3 The Dependence of Equilibrium Potential on DoC of EASP

There are several possible types of products forming during reduction of EASP. These various products differ in the nature of dependence of their EP upon DoC of EASP. For convenience and simplicity, the applicability of the Nernst equation to

<sup>3</sup> Lithium electrode  $\text{Li}^+ + e \rightleftharpoons \text{Li}$  in the discussed aprotic solutions is assumed to be at equilibrium state.

the systems described below is assumed, and the use of standard electrolyte solution is implied. Such approach does not affect the logic of exposition, but makes the description more illustrative. The four different EASP reduction products and the associated EP-DoC relationships are discussed below:

- i. Lithium is inserted into the host matrix forming solid solution of *lithium atoms* within certain composition range. An example of this product is lithium insertion into aluminum matrix; solid solution is forming up to  $9 \times 10^{-4}$  at % of lithium [29]). Aluminum does not participate in the electrochemical reaction but acts as a solvent in the second phase, i.e.,  $x\text{Li}^+ + \text{Al} + xe^- \rightleftharpoons x\text{Li}\{\text{Al}\}$ .<sup>4</sup> The product can be expressed by the gross formula  $\text{Li}_x\text{Al}$ , which corresponds to the solution of  $\text{Li}^0$  in aluminum with the resulting molar fraction of  $y = x/(1 + x)$ . The correlation between molar fraction and molar-volumetric concentration is nonlinear due to the dependence of the product density upon composition.

The potential-determining reaction is



and the corresponding Nernst equation takes the form

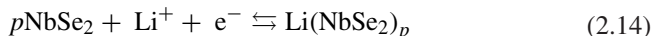
$$\varphi = \varphi_{\text{Li}^+/\text{Li}^0\{\text{Al}\}}^0 + \frac{RT}{zF} \ln \frac{c^\circ}{c} = \varphi' - \frac{RT}{F} \ln c \quad (2.13)$$

where  $c$  and  $c^\circ$  are concentration and standard concentration of lithium in aluminum, respectively, whereas  $z = 1$ .

The EP from (2.13) can be represented as the explicit function of the DoC utilizing the relationship  $y = cM_2/(cM_2 + \rho - cM_1) = x/(1 + x)$ , where  $M_1$  and  $M_2$  are molar masses of the solute (lithium) and solvent (aluminum), and where  $\rho$  is the solution density (a known function upon composition). Though  $d\varphi/d \ln x \neq RT/nF$ , the corrective factor can be easily calculated.

- ii. Lithium is inserted into the host matrix, forming solid solution and becoming a *part of a new, non-stoichiometric compound* within certain composition range. An example of this product is the formation of lithium niobium diselenide— $\text{Li}_x\text{NbSe}_2$  where solid solution is forming within the entire composition range ( $0 < x < 1$  [30, 31]):  $\text{NbSe}_2 + x\text{Li}^+ + xe^- \rightleftharpoons \text{Li}_x\text{NbSe}_2$

The potential-determining reaction is



In this case, the EP depends upon DoC according to formula:

$$\varphi = \varphi' - \frac{RT}{F} \ln \frac{1 - x}{x} \quad (2.15)$$

---

<sup>4</sup> Such case is not fully consistent with the previously given definition of EASP. This inclusion is justified by simplicity and completeness of the system description.

and

$$\frac{d\varphi}{d \ln x} = \frac{RT}{F} x(1-x)$$

That is, cases i and ii are *distinct using thermodynamic experimentation*.

- iii. Lithium is inserted into the host matrix, forming solid solution of *non-stoichiometric, lithium-containing compound dissolved in the host matrix*. Such result was proposed in the work of Pozin et al. [10] for the product of reduction of manganese (IV) oxide within the range  $0 < x < 1$ :  $\text{MnO}_2 + x\text{Li}^+ + xe^- \rightleftharpoons \text{Li}_x\text{MnO}_2$

The potential-determining reaction is



however, in reality, this process is best characterized by multiple equilibriums; different equilibrium achieved for each value of  $x$ . Accordingly, each point is characterized by a separate Nernst's equation:

$$\varphi = \varphi'(x) - \frac{RT}{F} \ln \frac{1-x}{x} \quad (2.17)$$

It is essential that the standard potential depends upon DoC:  $\varphi^\circ = \varphi^\circ(x)$ . Thus, the shift of EP is caused by the second (quantitative) component of the Eq. (2.17), and by the change of the standard potential due to the change of the nature of the product.

Similar phenomena are observed in liquid solutions where stepwise complex formation occurs. This solution can be characterized by the mean coordination number  $\bar{n}$  [32]. When the ligand-metal ratio changes (e.g., initially, solution contains only ligand in certain concentration  $[\text{L}]$ ; then, by titration, metal concentration  $[\text{M}]$  is increasing). In this case, both the total complex's concentration and mean coordination number undergo changes as the complex formation reaction proceeds. This process can be described as the change of the complex  $\text{ML}_{\bar{n}}$  concentration with simultaneous altering of its composition. The shift of the potential  $\Delta\varphi$  of metal (M) electrode versus the potential in the complex-free solution of metal ions is illustrated by the relationship

$$\Delta\varphi = \varphi^\circ(\bar{n}) - \frac{RT}{zF} \ln[\text{ML}_{\bar{n}}] \quad (2.18)$$

The physical meaning of this formula can be explained if the solvation of metal ions in highly concentrated electrolyte solutions (where concentration of metal ions is comparable to the reciprocal molar volume of the solvent) is considered instead of formation of complexes.

- iv. Lithium insertion leads to formation of a set of new solid products where *one or more product(s) is/are lithium-containing compound(s)*. An example of this set of products is the result of the reduction of copper(II) oxide [33]. In this case, the overall reaction is  $\text{CuO} + 2\text{Li}^+ + 2e^- \rightarrow \text{Cu} + \text{Li}_2\text{O}$  or, if copper(I) oxide is taken into account as intermediate product, the resulting reaction is:

$2\text{CuO} + 2\text{Li}^+ + 2\text{e}^- \rightarrow \text{Cu}_2\text{O} + \text{Li}_2\text{O}$ . Note that *one-directional arrows* connect the sides of the equations meaning that the reaction is irreversible. The formation of the set of products with various degree of lithiation is the most difficult case for electrochemical examination, due to several factors, listed subsequently. Let copper oxide transform according to the following scheme:  $\text{CuO} \rightarrow \text{Cu}_2\text{O} \rightarrow \text{Cu}$  with accompanying formation of  $\text{Li}_2\text{O}$ . While copper(I) oxide is forming, the chemical potential remains constant; dramatically changing only when copper(II) oxide is exhausted and metal copper begins appearing. For that reason, two plateaus of EP are expected on the potential versus time plot, with virtually instant transition from one to another. However, it is not clear if the EP can be established on the electrode comprised of stoichiometric compounds, such as  $\text{CuO}$ ,  $\text{Cu}_2\text{O}$ ,  $\text{Li}_2\text{O} \mid \text{Li}^+$ .

The second difficulty is the verification of the presence of the true dependence of EP upon the DoC, since the dependence may be merely weak and indistinguishable from the experimental noise. It will be shown in the next section of this chapter that the measurement of temperature coefficient of the EP can shed some light on this problem.

The last difficulty is inherently related to the feasibility of nonequilibrium electrochemical measurements, which will be discussed later. Even very small disturbance of the electrode equilibrated within the plateau (such as applying a few-mV potential step or harmonic wave, or low current pulse) dramatically changes the electrode's surface composition, easily bringing the composition outside of allowed limits.

However, if the equation of state is unknown (i.e., the Nernst equation is inadequate), it is difficult to determine by the shape of the  $\text{EP}(x)$  curve, which the type of the reaction (i–iv) takes place. The above reasoning demonstrates why another approach is necessary, namely carrying out the entropy measurements.

An illustration of the concepts discussed earlier is shown in Fig. 2.2 where an electrode  $\text{Li}_x\text{V}_2\text{O}_5 \mid \text{Li}^+$  reveals a number of features typical for EASP. The curve shows two areas where the OCV is almost independent upon composition with sharp transition from one domain to another. Two possible interpretations of this curve are

- (a) the electrode behaves according to the mechanism iv, considered previously, or
- (b) there exists a weak dependence of equilibrium potential on composition that has not been detected thus far.

### 2.3.4 Entropy of the Electrode Reaction

Solving a non-steady state problem of electrochemical kinetics means obtaining the relationships between current, potential, concentration, and time. Very often, these relationships can be found as the solutions of the differential equation known

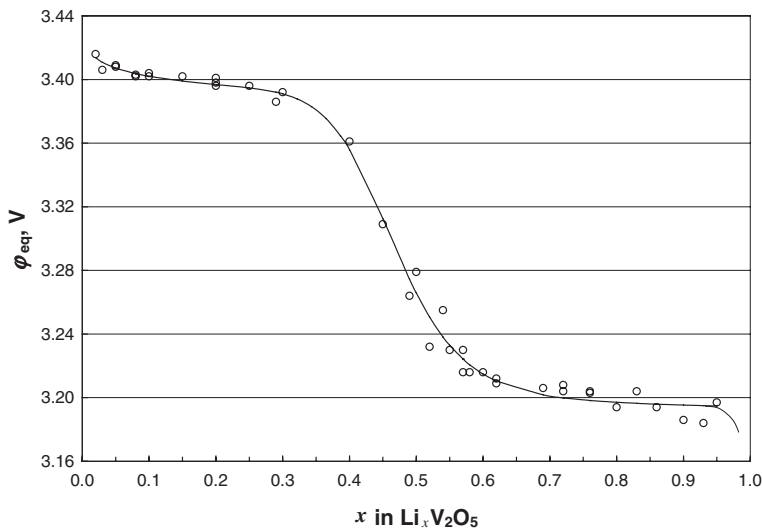


**Fig. 2.2** OCV of the cell Li | LiClO<sub>4</sub> (propylene carbonate) | Li<sub>x</sub>V<sub>2</sub>O<sub>5</sub> at various  $x$  at 22 °C [11]

as second Fick's law with corresponding initial and boundary conditions. The latter are either: the equation  $i = i(\varphi)$  or the relationship:  $\varphi = \varphi(c)$ , where  $i$  is the current density and  $\varphi$  is the electrode potential under load. The prior knowledge of the  $\varphi = \varphi(c)$  dependence is presumably known from theory or preceding experiment.

The calculation approach presented here deviates from this direct scheme for the sake of the full consideration given to the entropy of electrode reaction and showing the importance of simultaneous scrutiny of entropy and Gibbs energy. Entropy of the reduction/oxidation (or discharging/charging) process is an effective measure of these structural changes, including the possible phase transitions. Statistical thermodynamics provides the direct connection between the entropy ( $S$ ) and thermodynamic probability ( $w$ ), which is the numeric measure of the disarrangement of the system, by Boltzmann's equation  $w = \exp(S/k)$ , where  $k$  is Boltzmann's constant. Crystalline lattice, being characterized by certain symmetry degree, must be sensitive to its ordering-disordering caused by electrochemical insertion or extraction of guest species. A redox-reaction occurring in an electrochemical cell gives a unique opportunity to directly measure the cell's Gibbs energy and entropy.

According to the Gibbs-Helmholtz equation

$$\Delta S = -zF \frac{E}{T} \quad (2.19)$$

where  $E$  is the emf of the electrochemical circuit, particularly, of Eq. 2.1. Thus, the emf is equal to the EP ( $\varphi$ ) of the electrode under study in lithium scale (versus the Li | Li<sup>+</sup> reference).

Obviously, the entropy must depend on DoC of the electrode since the EP does:

$$\frac{\partial \Delta S}{\partial x} = -zF \frac{\partial(\phi/T)}{\partial x} = -zF \frac{1}{T} \frac{\partial \phi}{\partial x} \neq 0$$

Equation (2.15) with constant standard potential and (2.17) with the standard potential apparently depending on DoC can be rewritten in generalized form as

$$\phi = \phi^\circ + \Psi(T, x)$$

Equations (2.15) and (2.17) will then take the form

$$\phi(T, x) = \phi_1'(T) + \Psi_1(T, x) \quad (2.20)$$

and

$$\phi(T, x) = \phi_2'(T) + \Psi_1(T, x) \quad (2.21)$$

Then, it follows from Eq. 2.20 that

$$\frac{\partial \phi}{\partial T} = \frac{\partial}{\partial T} \phi_1^\circ(T) + \frac{\partial}{\partial T} \Psi_1(T, x)$$

or according to Eq. 2.19 (at  $E = \phi$ ),

$$\Delta S(T, x) = \Delta S_1^\circ(T) - zF \frac{\partial}{\partial T} \Psi_1(T, x)$$

Within a relatively narrow temperature range, far from melting point and far from the absolute zero, the derivative  $\partial E/\partial T$  is constant, i.e.,  $\partial^2 E/\partial T^2 = \partial \Delta S/\partial T = 0$ . If linear approximation is applied,  $\partial \Delta S^\circ/\partial T = 0$  and:

$$\Delta S(x) = \Delta S_1^\circ - zF \frac{\partial}{\partial T} \Psi_1(T, x) \quad (2.22)$$

Therefore,

$$\frac{\partial \Delta S}{\partial x} = -zF \frac{\partial^2}{\partial T \partial x} \Psi_1(T, y) \neq 0$$

because  $\partial \Delta S^\circ/\partial y = 0$  for the reaction (2.14).

In turn, dealing with the reaction (2.16), according to (2.21),

$$\frac{\partial \phi}{\partial T} = \frac{\partial}{\partial T} \phi_2^\circ(T) + \frac{\partial}{\partial T} \Psi_2(T, x)$$

In this case the result is

$$\Delta S(x) = \Delta S_2' - zF \frac{\partial}{\partial T} \Psi_2(T, x) \quad (2.23)$$

Oppositely to Eq. 2.15, here  $\partial \Delta S^\circ/\partial y \neq 0$ , that is why

$$\frac{\partial \Delta S}{\partial x} = \frac{\partial}{\partial x} \Delta S_2^\circ(x) - zF \frac{\partial^2}{\partial T \partial x} \Psi_2(T, x) = \frac{\partial}{\partial x} [\Delta S_2^\circ(x) - zF \Psi_2(T, x)] \quad (2.24)$$

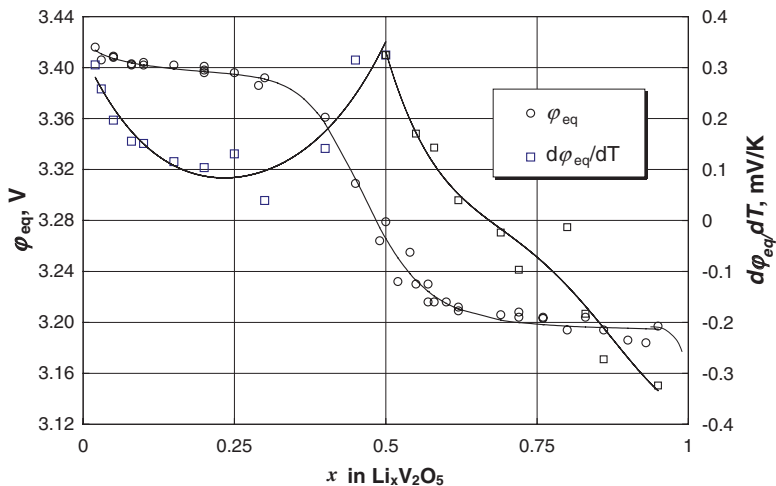


**Fig. 2.3** OCV of the cell  $\text{Li} \mid \text{LiClO}_4 (\text{propylene carbonate}) \mid \text{Li}_x\text{V}_2\text{O}_5$  at various  $x$  at 22 °C and its temperature coefficient  $d\phi_{eq}/dT$  [11]

It follows from Eq. 2.24 that  $\partial\Delta S/\partial x$  might be zero, in other words  $\Delta S_2^\circ - zF\Psi_2(T, x) = \text{const.}$  This may mean that the difference in standard entropies, that is, the difference in structures of different compounds  $\text{Li}_{p(x)}\text{Z}$  is entirely determined by lithium content, and no actual structural change occurred. Since determining of the *nature and composition* of the final product of the reaction can help to determine the *mechanism* of the reaction, the entropy calculations would be best supported by the structural and composition analyses.

In Fig. 2.3, the EP of  $\text{Li}_x\text{V}_2\text{O}_5 \mid \text{Li}^+$  electrode and the electrode's temperature coefficient are overlapped in a single chart. Distinct dependence of entropy upon composition allows concluding that instead of the “true” plateaus on the equilibrium curve, a weak dependence upon composition takes place. A sharp peak at  $x = 0.5$  most likely signals a phase transition at this composition.

## 2.4 Mass Transport in Solid Electrodes

Reduction (oxidation) of EASP begins with the enrichment (or depletion) of the surface layer with the product of the reaction (i.e., guest concentration change) followed by the guest distribution throughout the bulk of the material. The mechanism of distribution may vary, from the simple diffusion process to complicated multi-step solid-phase reactions including the formation of new phases. The following discussion is limited to the simple case of diffusive dissipation of inserted particles, and formation of the *phase of variable composition* (the solid solution).

For simplicity, the solid solution phase is considered nonporous and electronically conductive [34].<sup>5,6</sup> The latter assumption allows for absence of determination whether the guest entities are ions or atoms.

Diffusion occurring in solids during electrochemical processes never approaches steady state conditions. Therefore, only methods suitable for surveying of non-steady state electrochemical processes can be successfully employed for such investigations. The diffusion process follows second Fick's law

$$\frac{\partial C}{\partial t} = \nabla \cdot (D \nabla C) \quad (2.25)$$

or, for one-dimensional plane diffusion

$$\frac{\partial C}{\partial t} = \frac{\partial}{\partial x} \left( D \frac{\partial C}{\partial x} \right) \quad (2.25a)$$

where  $D = D(C)$  is the diffusion coefficient (DC) *depending on concentration*. The flux density  $j$  is defined by first Fick's law.

$$j = -D \nabla C \quad (2.26)$$

Equation 2.26 is correct in any case where the spatial concentration difference is sufficient to drive the mass transport.

The dependence of DC upon concentration immensely affects the solution of the related equations, such as the Eq. 2.25. Equation 2.25 has the *analytical solution* if  $D = \text{const}$ , which is true for many border conditions realized in actual electrochemical experiments. However, if the DC changes with concentration, the equation can be solved only numerically. Therefore, it is as useful and convenient to conduct the experiments within such conditions, where the DC changes are negligible. Equation 2.25a is then reduced to

$$\frac{\partial C}{\partial t} = D \frac{\partial^2 C}{\partial x^2} \quad (2.25b)$$

The practical implementation of such measurements is challenging. First, the surface concentration perturbation occurring during the measurement must be as small as possible. However, the physical meaning of “as small as possible” is different for each material and experimental method. Lithium-ion EASPs are composed of lithium, transient metals, oxygen, and, possibly, other elements. Molar volume of these materials is typically fraction of liter per mole. For example, molar volume of lithium cobalt oxide, which is the main cathode material for

---

<sup>5</sup> The assumption of electrode materials' conductivity is an intentional oversimplification. In reality, vast majority of lithium-ion electrode materials possess rather low conductivity and neglecting their resistance is incorrect in terms of the strictly mathematic approach to balancing the electrode equations. However, this simplified calculating approach is used for clarity in presentation of a novel concept. For the complete mathematics of transport phenomena pertaining to the simpler electrochemical systems, the reader is directed to J. Newman's book [34].

<sup>6</sup> For the same reasons, only plane diffusion is considered here.



commercial LIC, is  $19.45 \text{ cm}^3 \text{ mol}^{-1}$ . Lithium concentration in electrodes usually ranges up to few tens of moles per liter, rarely falling below several moles per liter. In  $\text{Li}_x\text{CoO}_2$ , the typical lithium concentration range is between  $\sim 20$  and  $51 \text{ mol L}^{-1}$ ; whereas in carbonaceous negative electrodes, the lowest lithium concentration approaches almost zero (at least at the surface), but also goes up to  $\sim 30 \text{ mol L}^{-1}$  in the fully lithiated state. A liquid solution with such content of solute is considered a concentrated solution experiencing “strong deviations from ideality” of physical and electrochemical properties. In particular, the dependence of the DC on concentration takes the form of Nernst-Hartley equation [35]

$$D = D_0 \left( 1 + \frac{\partial \ln \gamma}{\partial \ln C} \right) \quad (2.27)$$

As demonstrated in previous sections, Eq. 2.27 is out of the direct use due to absence of the data on the activity coefficients  $\gamma$  in EASP. Instead of Eq. 2.27, another equation that contains DC is more helpful, namely the Einstein-Smoluchowski relation (Eq. 2.28) for mean square distance  $\langle d^2 \rangle$  of a freely randomly walking particle during time  $t$ :

$$\langle d^2 \rangle = 2Dt \quad (2.28)$$

Equation (2.28) shows that any plane of constant concentration propagates proportionally to the square root of time. Based on the above considerations, Eq. 2.28 may serve the dual function: (a) it is useful for preliminary validation of the value of the experimentally obtained DC and (b) can be used for the preliminary estimation whether limited or semi-infinite diffusion model should be applied. These estimates are using the thickness of the sample and the experiment duration, as well as the predetermined possible range of DC values. For example, when experiment duration equals 1 h, a nonporous electrode with the thickness of few millimeters behaves as semi-infinite media when diffusion coefficients are greater than  $10^{-16} \text{ cm}^2 \text{ s}^{-1}$ .

One of the most important methods of testing of the EASPs is their *galvanostatic reduction and oxidation*. The analogous method in electroanalytical chemistry is called chronopotentiometry (CPM). In CPM, the *transient time* corresponds to the *utilization* of the battery electrode. The transient time is the time when the surface concentration of the depolarizer drops to zero; the utilization is the fraction of inserted (extracted) lithium atoms. Obviously, at constant current conditions the difference between these characteristics is solely a matter of units. However, since the guest's concentration varies from (sometimes) zero to a certain maximal value, the DC will suffer all possible variations as well, and all the CPM equations cannot be used, except the single CPM relationship given below.

The theory of the CPM shows that the reversible curves obtained at different currents ( $i$ ) obey the law:  $i^2\tau = \text{const}$  where  $\tau$  is the transient time. It has been shown with the help of the similarity theory that this rule covers any diffusion-controlled constant-flux process in semi-infinite media, and it works not only for transient time, but also for any time necessary to reach a certain potential regardless of the DC dependence upon concentration (or lack of thereof) [36].

*Potentiodynamic reduction and oxidation* (chronovoltammetry, CVA) is frequently (and sometimes, erroneously) employed for characterization of the processes on EASP with the accompanying formation of solid solution.<sup>7</sup> Very often, the equations for diffusion kinetics in semi-infinite media (Randles-Sevcik, Matsuda-Ayabe, and other [28]) are employed for interpreting the results obtained via linear sweep of potential with the rate of  $5\text{--}15\text{ mV s}^{-1}$  within the potential range of the electrode's OCP. However, these equations have been derived for constant DC, and do not apply in the above conditions. Even if the DC were constant, the approach is not relevant to the measurements associated with the EASP reduction, or lithium insertion. Indeed, *no Li-ion diffusion-related maximum appears* on the CVA-gram. The CVA current corresponding to insertion is an *infinitely increasing function*. The experimentally observed maxima are determined by other phenomena, different to that occurring in classic CVA (e.g., reaching the maximum of allowed guest's concentration, or new phase formation).

Regardless of the measurement technique, a common approach exists to address the lack of constant DC throughout the entire range of concentration (potential). It is possible to establish the intervals where the DC is constant. From the knowledge of the DC's dependence upon concentration within these intervals, the DC behavior for overall concentration range can be determined. Based on this approximation, an entire group of the applied electrochemical analyses methods have been enabled.

These electrochemical non-steady state methods are divided into three groups, where potential, current, or charge drive the process. The driving (controlling) factors in turn define the border and initial conditions for solving Eq. 2.25b [28]. The representatives of each group are described in the following section. All experiments must be performed on an electrode made of partially discharged EASP in lithium-ions containing solutions, initially at equilibrium potential. The initial concentration of lithium in the solid is denoted as  $c_0$ , and the current density  $i$  is used as the rate of the reaction, unless otherwise noted. The ionic transport in the solution is typically significantly faster than the diffusion within the solid, thus the electrolyte concentration can be assumed constant during the short-term experiment.

### 2.4.1 Galvanostatic Pulse Method

In the galvanostatic pulse method (GSPM) [37], lithium is inserted into (and extracted from) the surface layer of the electrode by a short rectangular current pulse  $i$ . The charge transfer step is presumed fast and the measured electrode potential is entirely determined by the surface concentration of lithium. During the

---

<sup>7</sup> The experiments with ultra-low scan rates (few microvolts per second) are beyond the scope of this paragraph but will be touched upon later, in Sect. 2.7.

experiment, the potential initially leaps to a certain maximal (minimal) value and then gradually returns to the initial value. The amount (in mol per area unit) of inserted lithium is  $n = it/F$ . Strictly speaking, the pulse should be instantaneous ( $t \rightarrow 0$ ). However, in practice, the sufficiently short pulse duration is less than the characteristic time of the diffusion.

The solution of Eq. 2.25b with initial  $c(0, x) = c_0$  and border  $(\partial c/\partial x)_{x=0} = 0$  (interface),  $c(t, \infty) = c_0$  (bulk) conditions for  $x = 0$  is [38]:

$$c(t, 0) = c_0 + \frac{i\tau}{F\sqrt{\pi Dt}} = c_0 + At^{-1/2} \quad (2.29)$$

Here,  $\tau$  is the pulse duration; the current  $i$  is positive for insertion and negative for extraction.

The DC can be calculated from the slope of the line illustrating the relationship of  $c$  versus  $t^{-1/2}$ . However, the observed value is the potential, which is a function of concentration  $\varphi = \varphi(c)$ . If the dependence of potential on concentration is of Nernst's type Eq. 2.29 takes the form

$$\exp \left[ \frac{F}{RT} \Delta\phi(t) \right] = 1 + \frac{A}{c_0} t^{-1/2} \quad (2.30)$$

where  $\Delta\phi(t) = \varphi(t) - \varphi_{eq}$ . For all EASP materials, the concentration must be expressed as a function of equilibrium potential.

The main disadvantage of the current pulse method lies in the ambiguous validity of the results. The ambiguity is caused by several factors. First, the requirement that  $t \rightarrow 0$  leads to the inversely proportional current increase, and may cause substantial concentration and/or the DC changes within the surface layer. These changes negate the application of Eq. 2.25b. Secondly, extending the pulse duration alters the experiment conditions while distorting the border condition of  $x = 0$ , thus rendering Eq. 2.29 inadequate. Appropriate balancing of these equations (Eqs. 2.25b and 2.29) needs the preliminary knowledge in the DC value. An estimate of the allowed pulse time can be obtained using Eq. 2.28. Another requirement is the shallow penetration of guests into the host lattice. If the penetration depth  $d$  corresponds to 2–3 atomic diameters, then for the ion  $O^{2-}$  with the ionic radius of  $(1.5\text{--}1.7) \times 10^{-8}$  cm, [39]  $d \approx 1$  nm. In this case, the allowed pulse duration is 0.05 and 500 ms for diffusion coefficient values between  $10^{-10}$  and  $10^{-14}$  cm<sup>2</sup> s<sup>-1</sup>. If lithium content change in such thin surface layer is 1 % (for example, in LiCoO<sub>2</sub> this corresponds to  $\Delta c = 0.5$  mol L<sup>-1</sup>). The resulting allowed pulse current density will fall between 100 and 10  $\mu\text{A cm}^{-2}$ .

In materials with high diffusion coefficients ( $D > 10^{-11}$  cm<sup>2</sup>/s), the pulse current methods do not yield accurate results. This inaccuracy is caused by both technical and fundamental difficulties. The former problem is associated with the limited capabilities of the pulse generators. The latter problem is related to the speed of the double layer charging, where the fraction of 50  $\mu\text{s}$  for the pulse duration might be not sufficient to achieve the double layer charging.

### 2.4.2 Potential Transient Method

In this method, [37] an electrode at equilibrium is polarized by a small shift of potential, thus keeping a constant concentration of inserted atoms on the surface of the electrode. The DC can be calculated from the registered current-versus-time curve called chronoamperogram. The method is also called single-step chronoamperometry (SSCAM). In this method, the condition  $D \approx \text{const}$  is under better control than in the GSPM.

The solution of Eq. 2.24b for semi-infinite electrode at initial  $c(0, x) = c_0$  and border  $c(t, 0) = c_s$  and  $c(t, \infty) = c_0$  conditions has the form

$$\frac{c - c_s}{c_0 - c_s} = \text{erf} \frac{x}{2\sqrt{Dt}} \quad (2.31)$$

while the current density

$$i = FD \left( \frac{\partial c}{\partial x} \right)_{x=0} = F(c_s - c_0) \sqrt{\frac{D}{\pi t}} \quad (2.32)$$

The height of the potential step is defined by the function  $\varphi = \varphi(c)$ . The preference for the low value of the potential step is related to the following causes: (a) the effect of the small potential step on the value of the DC is small, and (b) the dependence of the potential upon “guest” concentration can be simplified to linear relationship:  $c_s - c_0 = \Delta\varphi$ . Thus, the current decrease remains linear versus reciprocal square root of time ( $t^{-1/2}$ ).

For the electrode of limited thickness  $\delta$ , the border condition  $c(t, \infty) = c_0$  must be substituted with  $(\partial c / \partial x)_{x=\delta} = 0$  (impenetrable border). The expression for the current density then obtains a more complicated form, which can be found in a handbook dedicated to the mathematics of diffusion [39]. However, the sample can be considered as infinite if the dimensionless parameter  $Dt/l^2 < 0.3$ .

In such case, the calculation of DC is simple. The criterion for infinite sample dimensions yields that the largest possible  $D = 10^{-8} \text{ cm}^2/\text{s}$ . Thus, the electrode of 60  $\mu\text{m}$  thickness behaves as semi-infinite during the  $10^3 \text{ s}$  current decay. Therefore, if the experiment’s duration is limited to few minutes ( $10^2 \text{ s}$ ) then the allowed sample thickness would be  $\sim 20 \mu\text{m}$ . Such consideration is necessary when film or single-crystal electrodes are employed.

The examples of the described methods’ applications can be found in the works by Nikolskaya et al. [14] where DC of lithium in niobium diselenide of layered structure  $2H\text{-NbSe}_2$ <sup>8</sup> has been determined by GSPM and SSCAM. For calculations,

---

<sup>8</sup> This material has the metallic type of conductivity and extremely flexible crystalline lattice (the lattice can expand along the  $c$  axis, doubling the parameter), and can be easily pressed into pellets. The degree of lithium-ion reduction is about 0.7 (i.e., lithium in the crystal is present in 70 % as atoms and 30 % as ions). Thus, layered niobium diselenide is the perfect material for testing the proposed models. In order to eliminate the pores, pellets have been impregnated with molten paraffin-polyethylene alloy under vacuum in all cited works.

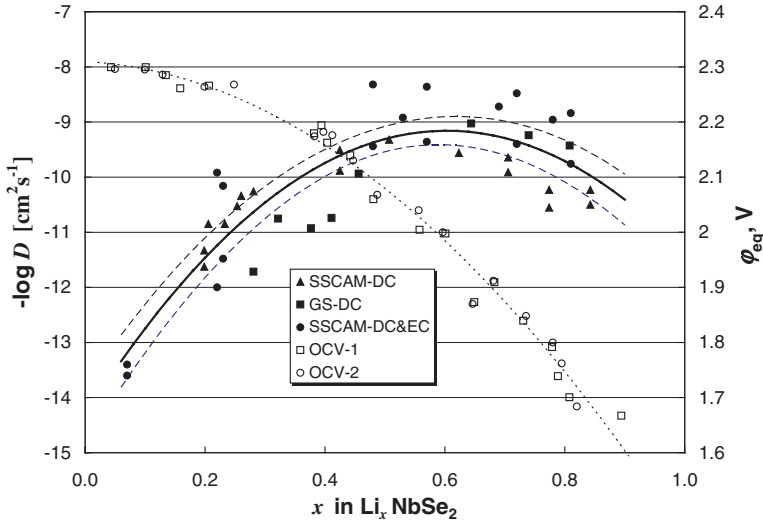


**Fig. 2.4** OCV of the cell:  $\text{Li} \mid 1 \text{ M LiClO}_4 \text{ (PC)} \mid \text{Li}_x\text{NbSe}_2$ ; DC of lithium at various  $x$ . The accuracy of the DC calculation was 0.2–0.3 in the order of magnitude ( $\pm 1.6$ – $2.0$  in mantissa); dashed lines show 95 %—confidence interval. References OCV-17; OCV-2 [12]; SSCAM-DC and GS-DC [14]; SSCAM-DC and EC [15]

the equilibrium curve was obtained. The experimental results are well consistent between various measurement methods (Fig. 2.4). The DC varies from  $10^{-11}$  to  $10^{-9} \text{ cm}^2 \text{ s}^{-1}$  passing over a maximum at  $x \approx 0.5$ – $0.6$ . This is the region where the interlayer distance reaches the maximum [40] not changing with further lithium content increase. However, the number of available diffusion leaps decreases, which leads to the DC decrease.

The DC calculations did not include any assumption of the concentration dependence of the DC. Comparing the DC and OCV curves, it is easy to ascertain that there is no direct proportion between  $f_1 = \frac{\partial \phi(x)}{\partial \ln x}$  and  $f_2 = D(x)$ , which should exist due to Eq. 2.27. Thus, from Nernst's equation:

$$\phi = \text{const} - \frac{RT}{F} \ln \gamma c$$

where  $\gamma$  is the activity coefficient, it follows that

$$\frac{\partial \ln \gamma}{\partial \ln c} = \frac{F}{RT} \frac{\partial \phi}{\partial \ln c} - 1$$

The above constitutes another reason for avoiding the term of activity in studying the EASP.

## 2.5 Rate of Electrochemical Stage

The rate  $i$  of the electrochemical reaction depends on reactants' concentrations  $c$ , temperature  $T$ , and electrode potential  $\phi$ . For mono-molecular process,

$$i = k(T, \phi)c \quad (2.33)$$

where  $k(T, \phi)$  is the rate constant. Some authors prefer using thermodynamic activity instead of concentration in the equations of the same type as Eq. 2.33. Previous sections of this text (Part 2.1) demonstrated that there was no viable reason for involving the concept of activity in thermodynamic considerations of EASP electrodes. Similarly, there are no reasons to use the activity in kinetic reactions [41].<sup>9</sup>

The necessary but not exclusive condition for the reaction to occur is the collision of particles, or the act of particles hitting the surface of another phase. Equation 2.33 reflects the assertion that the rate is directly proportional to the frequency of collisions. For a decomposition reaction, the number of bond breakages per unit of time is proportional to total number of particles.

However, not every collision leads to the product formation since many collisions are elastic. The collective efficiency of collisions is described by the reaction's rate constant. The rate constant depends on temperature and potential and on various environment factors, such as the *nature* of the solvent and electrolyte, and the *quantitative composition* of electrolyte solution.

## 2.6 Concentration Dependence of Exchange Current on EASP

In order to perform the relevant kinetic calculations, first, a specific mechanism of the reaction must be presumed. Thus, the process rate (expressed as current density<sup>10</sup>) of a single-step one-electron redox-reaction:



obeys the theory of mixed kinetics when both charge transfer and diffusion control the overall rate of the reaction (Butler-Volmer equation, BVE):

$$i = i_0 \left[ \frac{c_{\text{Ox}}^S}{c_{\text{Ox}}} \exp(-\alpha n \vartheta \eta) - \frac{c_{\text{Red}}^S}{c_{\text{Red}}} \exp(\beta n \vartheta \eta) \right] \quad (2.35)$$

<sup>9</sup> In the absolute reaction rate theory, the rate of the reaction is proportional to the concentration of activated complex, which is in equilibrium with reactants. Thus, the activated complex concentration can be calculated using the corresponding equilibrium constant and, consequently, the activities. This is the reason why the activity coefficients appear in kinetic equations.

<sup>10</sup> Unless otherwise noted, the term "current" is equivalent to the "current density" in the following text.

where  $i_0$  is the exchange current,  $\alpha$  and  $\beta$  are cathode and anode transfer coefficients ( $\alpha + \beta = 1$ ),  $\eta = \varphi - \varphi_{eq}$ —polarization,  $\vartheta = F/RT$ . The index “s” marks surface concentrations of both forms of the depolarizer. In fact, the observed current is the difference  $i = \vec{i} - \overleftarrow{i}$  between the currents of direct  $\vec{i}$  and reverse  $\overleftarrow{i}$  processes of (2.24). The formulas for partial currents  $\vec{i} = nFk^\circ c_{Ox} \exp[-\alpha n\vartheta(\phi - \phi^\circ)]$  and  $\overleftarrow{i} = nFk^\circ c_{Ox} \exp[\beta n\vartheta(\phi - \phi^\circ)]$  include standard rate constant  $k^\circ$ , and the potential is counted from the standard potential value ( $\phi^\circ$ ) for the reaction (Eq. 2.34). The dependence of the exchange current on concentration is usually expressed as

$$i_0 = i_0^\circ c_{Ox}^\beta c_{Red}^\alpha, \quad (2.36)$$

where  $i_0^\circ$  is the *standard exchange current* having the following dimensionality: (current)  $\times$  (length)/(matter amount), e.g., A cm mol<sup>-1</sup>. However, the formula (Eq. 2.36) is applicable only in case of the Nernst-type potential behavior being derived from the equation

$$i_0 = nFk^\circ c_{Ox} \exp[-\alpha n\vartheta(\phi_{eq} - \phi^\circ)] = nFk^\circ c_{Red} \exp[\beta n\vartheta(\phi_{eq} - \phi^\circ)] \quad (2.37)$$

when  $\phi = \phi^\circ + \frac{RT}{nF} \ln \frac{c_{Ox}}{c_{Red}}$ . Then  $i_0^\circ = Fk^\circ c_{Ox} \exp\left(-\alpha \frac{nF\phi^\circ}{RT}\right)$

If  $\varphi = \varphi(c)$  is not expressed by the Nernst equation, then  $\vartheta \neq F/RT$ . Indeed, at equilibrium ( $\varphi = \varphi_{eq}$ ) the currents of direct and reverse reactions are equal,  $i = 0$ , and

$$c_{Ox} \exp[-\alpha n\vartheta(\phi_{eq} - \phi^\circ)] = c_{Red} \exp[\beta n\vartheta(\phi_{eq} - \phi^\circ)] \quad (2.38)$$

In logarithmic form (Eq. 2.38)

$$\phi_{eq} = \phi^\circ + \frac{1}{(\alpha + \beta)n\vartheta} \ln \frac{c_{Ox}}{c_{Red}} \quad (2.38a)$$

if  $\vartheta = F/RT$ , then the entire relationship (Eq. 2.37) can be reduced to the form equivalent to the Nernst's Eq. (2.38a).

It follows from Eq. (2.36) that increasing of concentration of both oxidized and reduced forms leads to the increase in exchange current. Oppositely, taking logarithm and the derivative in respect to  $c_{Red}$  of the second equation (Eq. 2.37) the following can be derived:

$$\frac{d \ln i_0}{d \ln c_{Red}} = 1 + \beta \phi_{eq} \frac{d\vartheta}{d \ln c_{Red}} \quad (2.39)$$

since  $\vartheta = 1/(l\partial\varphi_{eq}/\partial \ln c)$ .

It follows from (Eq. 2.30) that the exchange current increases if  $\frac{d\phi_{eq}}{d \ln c_{Red}} > -\frac{RT}{\beta nF}$ , and decreases in the opposite case.

In the phenomenological theory the transfer coefficient is an empirical quantity, which is usually equal to 0.5, and is not dependent on the concentration and the potential (the Brønsted-Polanyi-Semenov principle). Therefore, experimental testing of the proposed approach should provide an answer, in particular, to the question of whether the principle is obeyed in this case.

In physical sense, the substitution of  $F/RT$  with  $1/(l\partial\varphi_{eq}/\partial \ln c)$  is relative to the logical device realized in the VTF model of the conductivity (see Chap. 3) where,

in fact, the absolute zero temperature is substituted with a sort of “relative zero temperature”: the  $T_0$  temperature (Eq. 3.3) is the temperature at which the ions mobility ceases to exist. Similarly, the value of  $1/|\partial\varphi_{eq}/\partial\ln c|$  can be interpreted as the “ $F/r(c)T$ ” where the absolute gas constant  $R$  is substituted with a “relative gas constant  $r$ ” depending on concentration  $c$  and is specific to a given material.

## 2.7 The Methods of Investigation of Electrochemical Reaction Step

The step of charge transfer in the multi-step process of electrochemical reduction and oxidation of EASP is relatively fast. Reliable data on the kinetic parameters of this step (exchange current or rate constant and transfer coefficient) can be established by using high-frequency methods examining short-term response of the electrode, with experiment times being much shorter than these allowed for studying of the diffusion step. The requirements for minimal perturbation are the same as those recommended for diffusion investigations. However, at early stages of electrode disturbance, the double-layer capacity ( $C$ ) can affect the results, and together with high resistance of the EASP electrodes ( $R$ ), lead to high value of the *time constant* ( $RC$ ) of the electrochemical cell. The high value of  $RC$  is capable of distorting the high-frequency experimental results.

Many electrochemical analytical *combined methods* allow for simultaneous calculation of DC, exchange current (EC), and transfer coefficients. For example, in a method called the coulostatic or charge-step method [28] a current pulse of 0.1–1  $\mu\text{s}$  is applied to the electrode, and the variation of the electrode potential with time after the pulse (that is, at *open circuit*) is recorded. The method is very similar to GSPM; however, the instrumentation is different, namely, the charge is injected by discharging a small capacitor across the electrode. The results are not affected by the double-layer capacity and electrode resistance.

The SSCAM is the most advantageous method due to the reasons given in Part 2.2. However, to get consistency of the DC values calculated from the results of combined methods and from the experiments where the diffusion exclusively controls the overall rate, the experimental values of  $\vartheta = d\varphi_{eq}/d\ln c$  must substitute the  $\vartheta = nF/RT$  in the BVE.

The equation for mixed kinetics in SSCA, has the form [42]

$$i(t) = I(0) \exp(\lambda^2 t) \text{erfc}(\lambda \sqrt{t}) \quad (2.40)$$

where  $I(0)$  and  $\lambda$  are the formal parameters

$$I(0) = i_0 [\exp(-\alpha \vartheta \eta) - \exp(\beta \vartheta \eta)] \quad (2.41)$$

and

$$\lambda = i_0 \frac{\exp(\beta n \vartheta \eta)}{n F c_0 \sqrt{D}}. \quad (2.42)$$



For simplicity, the latter equation neglects the diffusion limitations in the liquid phase. The two limiting cases, when  $t \rightarrow 0$  and  $t \rightarrow \infty$ , yield from Eq. 2.30:

$$i(0) = I(0)$$

which corresponds to the pure sluggish charge transfer reaction, and

$$i(\infty) = \frac{I}{\lambda} \frac{1}{\sqrt{\pi t}}$$

This is, in fact, Eq. 2.31.

Toroshchina et al. have conducted the SSCAM experiments with  $\text{Li}_x\text{NbSe}_2$  and  $\text{Li}_x\text{V}_2\text{O}_5$  [15]. Small potential signal ( $\pm 4$ –12 mV) was applied to the electrode  $\text{L}_x\text{Z} \mid 1 \text{ M LiClO}_4$  (PC) at equilibrium at various degree of discharge, and the response chronoamperogram was registered during 100–200 ms. The formal kinetic parameters  $I(0)$  and  $\lambda$  have been determined by fitting the experimental curves to Eq. 2.40 by the nonlinear least-squares method, and the real parameters have been calculated from Eqs. 2.41 and 2.42.

The obtained DC values, presented in Fig. 2.4, labeled as “SSCAM-DC&EC” demonstrate good agreement between the results obtained by different methods.

To find the EC and transfer coefficient, Eq. 2.41 has been converted into two convenient forms proposed by Essin in 1940 [42].

$$\log J_+ \equiv \frac{i}{1 - \exp(\vartheta \eta / RT)} = \log i_0 - \alpha \vartheta \eta$$

and

$$\log J_- \equiv \frac{i}{\exp(-\vartheta \eta / RT) - 1} = \log i_0 + \beta \vartheta \eta$$

Both  $\log J_+$  and  $\log J_-$  linearly depend upon polarization  $\eta$ , and the both transfer coefficients can be calculated from the slope of the straight lines (Fig. 2.5). The experimental value of  $\vartheta$  has been used in all calculations. The relation  $\partial \eta / \partial \ln J_{\pm} = 2(\partial E_{eq} / \partial \ln c_{Red})$  means that  $\alpha = \beta = 0.5$  is satisfactorily fulfilled and does not depend on  $x$ .

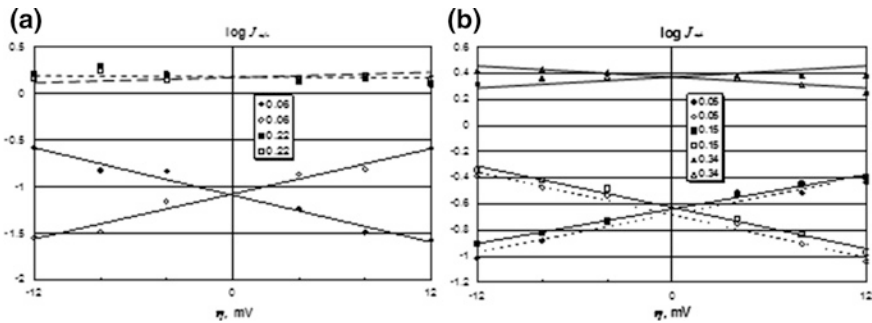


**Fig. 2.5** Polarization curves in Essin's coordinate set for  $\text{Li}_x\text{NbSe}_2$  (a) and  $\text{Li}_x\text{V}_2\text{O}_5$  (b)

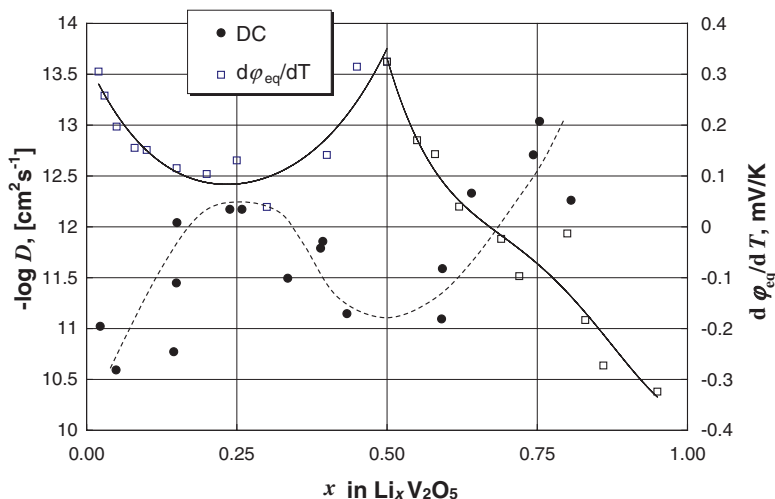


**Fig. 2.6** Diffusion coefficient of lithium in  $\text{Li}_x\text{V}_2\text{O}_5$  at various temperatures, and entropy of the reaction of insertion

The composition dependence of the diffusion coefficient of lithium in the lithium vanadate  $\text{Li}_x\text{V}_2\text{O}_5$  has a complicated character (Fig. 2.6). The extremes on the DC— $x$  the entropy— $x$  curves appear at the same values of  $x$ , which is not surprising since both parameters are connected to the material structure. Calculation of the DC from SSCAM experiment using  $\vartheta = nF/RT$  did not reveal such correlation indirectly confirming the rationality of the developing approach.

In contrast to the case of the diffusion coefficients, a direct relationship with the structure is not that obvious for the exchange current. However, the calculations also reveal a relationship between the course of the entropy versus composition plots and the exchange current versus composition plots (Fig. 2.7): in the region where one phase exists (region  $x < 0.5$  or  $x > 0.5$  for  $\text{Li}_x\text{V}_2\text{O}_5$ , and the entire range of  $x$  for  $\text{Li}_x\text{NbSe}_2$ ) the curves are monotonic, and phase transformations cause changes in their character. The results shown in Figs. 2.6 and 2.7 stand in contrast

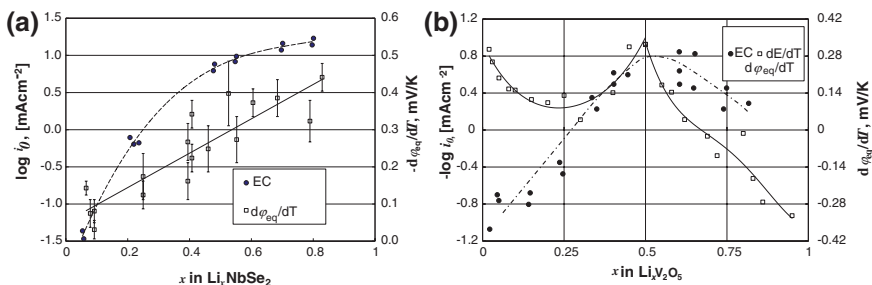


**Fig. 2.7** Exchange current at various  $x$  on  $\text{Li}_x\text{NbSe}_2$  (a) and  $\text{Li}_x\text{V}_2\text{O}_5$  (b)

to some published work [43–46], where calculations were performed without consideration of the *experimental dependence* of the equilibrium potential on  $x$ . Such approach did not reveal dependence of  $i_0$  on the composition of the solid phase. In particular, the authors of the work [43] have not found any effect of lithium content in  $\text{Li}_x\text{NbSe}_2$  on exchange current, despite such effect being in existence.

## 2.8 Selected Examples of OCP and Related Dependencies on Lithium Content

In the previous parts of this chapter, few typical OCV curves have been described from the phenomenological point of view. Besides the curves presented here, numerous measurements of the OCP have been published for various materials; thus covering the full spectrum of possible types of equilibrium potential versus composition curves.

J.D. Raistrick et al. [2, 6] were perhaps the first who studied the thermodynamics of electrochemical insertion of lithium into EASP. In these works, Gibbs energy and entropy of lithiation of tungsten and vanadium bronzes have been measured along with the determination of lithium diffusion coefficient.<sup>11</sup> The OCP and entropy curves of  $\text{Li}_x\text{Na}_{0.56}\text{WO}_3$  were smooth, confirming formation of the solid solution within the interval  $0.0004 < x < 0.35$ . However,  $d\varphi_{\text{eq}}/dx \neq d\Delta S/dx$ , similarly to the case of  $\text{Li}_x\text{NbSe}_2$  where the OCP curve can be approximated by a parabolic curve (Fig. 2.4), while the  $\Delta S - x$  dependence is linear (Fig. 2.7a).

Figure 2.8 represents the OCV and its temperature coefficient corresponding to the process of lithium insertion into electrochemically deposited manganese (IV) oxide [10]. In the area  $x < 0.7$ , the OCP demonstrates strong dependence upon lithium content, while the temperature coefficient remains constant. The interpretation of such peculiar phenomenon follows the case iii mechanism in Part 2.2.3.

Formation of a stage structure during lithium intercalation into graphite is a commonly recognized phenomenon and was touched upon in Chap. 1 of this book, in the section dedicated to carbonaceous anodes [47]. The OCP and entropy diagrams presented in Fig. 2.9 are perfectly consistent with the staging model. The areas where both entropy and Gibbs energy do, or do not depend upon lithium concentration, coincide with the corresponding composition ranges of different phases (stages).

Figure 2.10 presents the thermodynamic and crystallographic properties of lithium nickel cobalt oxide  $\text{Li}_x\text{Ni}_{0.8}\text{Co}_{0.2}\text{O}_2$ .<sup>12</sup> The entropy curve is consistent with

<sup>11</sup> The diffusion coefficients found in the  $\text{Li}_x\text{Na}_{0.56}\text{WO}_3$  bronzes are of the order of magnitude from  $10^{-9}$  to  $10^{-7} \text{ cm}^2 \text{ s}^{-1}$ . Such a high values of the DC would eliminate the rate-capability limitations of the cathode material. So far, however, the high-rate LIB with tungsten bronze-based anode has not been reported.

<sup>12</sup> Mars rovers “Spirit” and “Opportunity” as well as other speciality battery consumers employ lithium-ion batteries with cathodes based on this material.

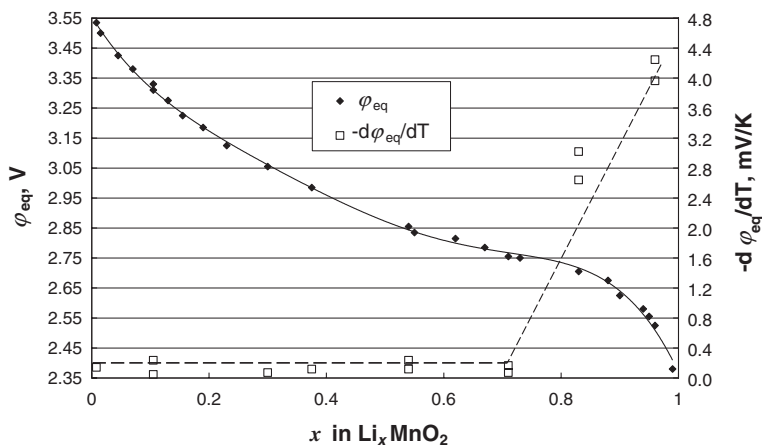


**Fig. 2.8** OCV of the cell  $\text{Li} \mid 1 \text{ M LiClO}_4 \text{ (PC)} \mid \text{Li}_x\text{MnO}_2$  at various  $x$  at  $20^\circ\text{C}$  and its temperature coefficient  $d\phi_{eq}/dT$

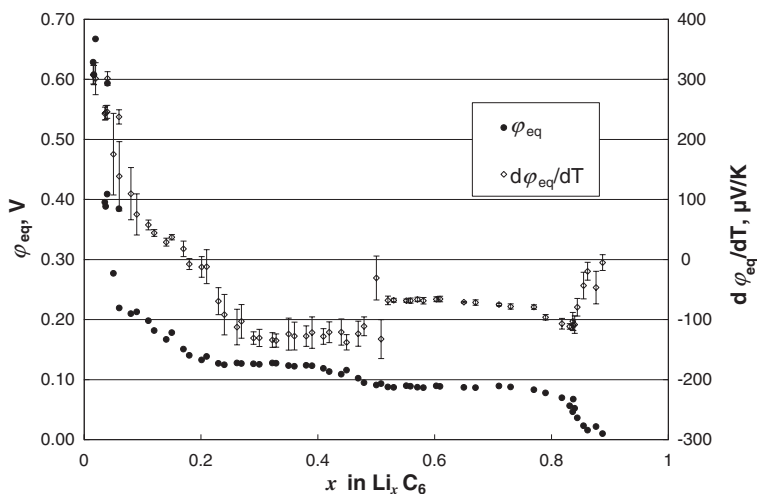


**Fig. 2.9** OCV of the cell  $\text{Li} \mid 1 \text{ M LiPF}_6 \text{ (carbonates blend)} \mid \text{Li}_x\text{C}_6$  at various  $x$  at  $20^\circ\text{C}$  and its temperature coefficient  $d\phi_{eq}/dT$

the direct crystallographic measurements. Thus, three areas of the curve can be highlighted. There is a peak at  $x \approx 0.85$ , and a plateau at approximately  $0.4 < x < 0.55$  where  $\Delta S \approx 0$ . The peak indicates that a phase transition develops in the concerned composition region, while in the plateau area no changes in the crystalline lattice are observed. At  $0.2 < x < 0.3$ , the entropy slightly increases and remains constant at  $x < 0.3$ . From this approach, it follows that the cathode

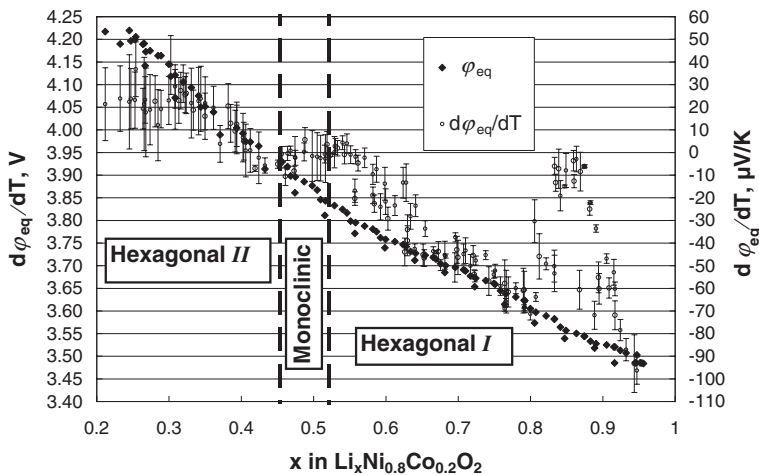


**Fig. 2.10** OCV of the cell  $\text{Li} \mid 1 \text{ M LiPF}_6 \text{ (carbonates blend)} \mid \text{Li}_x\text{Ni}_{0.8}\text{Co}_{0.2}\text{O}_2$  at various  $x$  at  $20^\circ\text{C}$  and its temperature coefficient  $d\phi_{\text{eq}}/dT$ ; [48] areas of different crystalline structures determined by XRD are indicated. Unpublished Yardney internal R&D project

material experiences the greatest impact during the last period of the charge where the electrode potential drops below  $\sim 3.6$  V. From these measurements it is apparent that the smallest effect on the crystalline lattice is observed when the potential of cathode material changes from  $\sim 3.8$  to  $4.0$  V, i.e.,  $x$  in  $\text{Li}_x\text{Ni}_{0.8}\text{Co}_{0.2}\text{O}_2$  varies from  $\sim 0.35$  to  $0.55$ . In this region, the electrode delivers about 25–30 % of the full capacity. The practical confirmation of the OCP curves was done in large, manufacturing-type cells (25 Ah) developed for an orbiter application by Yardney Technical Products, Inc. The cells were charged to 3.9 V and discharged at C/2 rate during 1 h. After 25,000–30,000 cycles, their 100 % DOD capacity was 87–90 % of the initial.

Finally, with Fig. 2.11 taken as an example, the method called “dynamic capacity” is discussed [49] When employing the methods of investigation of the EASP, some researchers use the CVA at extremely low scan rates, down to few microvolts per second. It is suggested that at such rate, no concentration gradient forms in the solid material, and the insertion proceeds at quasi-equilibrium conditions. The value  $i/v$  is called the dynamic capacity ( $v$  is the potential scan rate), and is equivalent to the derivative  $dx/d\phi_{\text{eq}}$ . It is believed that the analysis of the  $dx/d\phi_{\text{eq}}$  versus  $\phi_{\text{eq}}$  allows determining the points of phase transitions.

Overlapping of two curves  $dx/d\phi_{\text{eq}}$  and  $d\phi_{\text{eq}}/dT$  demonstrates that two extremes on the former curve (at  $\phi_{\text{eq}} \approx 3.55$  and  $3.60$  V) match the peaks on the entropy curve. However, the well-shaped peak at  $\phi_{\text{eq}} \approx 3.70$  V on the  $dx/d\phi_{\text{eq}} - \phi_{\text{eq}}$  curve most likely *does not* correspond to a phase transition. Further, there is no indication of possible phase transitions at  $\phi_{\text{eq}} > 3.9$  V, which is prominent on the  $d\phi_{\text{eq}}/dT - \phi_{\text{eq}}$  curve.

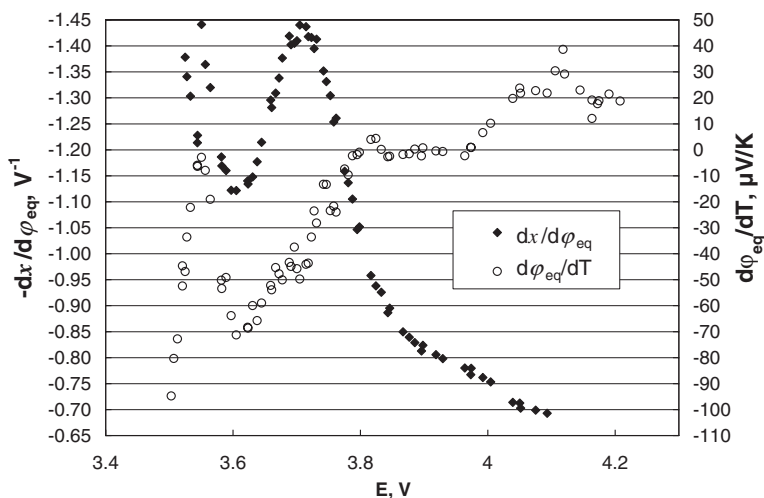


**Fig. 2.11**  $dx/d\varphi_{eq}$  and  $d\varphi_{eq}/dT$  versus OCV for the cell  $\text{Li} \mid 1 \text{ M LiPF}_6 \text{ (carbonates blend)} \mid \text{Li}_x\text{Ni}_{0.8}\text{Co}_{0.2}\text{O}_2$  at various  $x$  at 20 °C

## 2.9 Conclusion

Modeling of the processes occurring in lithium ion batteries during cycling is impossible without knowledge of fundamental thermodynamic and kinetic properties of the electrode materials. The chapter offered an approach for interpreting the dependencies of thermodynamic functions, and determining kinetic parameters of the reaction of electrochemical insertion–extraction of foreign ions into solid materials.

The chapter intentionally avoided appealing to the detailed microscopic description of the materials and mechanisms of the reactions trying to show the self-sufficiency of pure electrochemical methods for achieving the goals defined as collection of the data necessary for modeling lithium-ion batteries.

**Acknowledgments** The author is solely responsible for all errors, inconsistencies, misinterpretations, misconceptions, omissions, etc. The author expresses his greatest and warmest gratitude to his teachers: Prof. Adolph A. Ravdel and Prof. Konstantin I. Tikhonov, and to his friends and colleagues: (in alphabetic order) Dr. B.G. Karbassov, Dr. E.Yu. Nikolskaya, Dr. M.Yu. Pozin, Dr. S.I. Shustova, Dr. I.A. Srago, Dr. E.I. Toroshchina, Ms. S.A. Trebukhova, and Dr. E.G. Vinogradova-Volzhinskaya whose great contribution made this review possible.

## References

1. Modified after Encyclopaedia Britannica. Accessed on July 17, 2013, <http://www.britannica.com/EBchecked/topic/264278/heterogeneous-reaction>
2. Raistrick ID, Mark AJ, Huggins RA (1981) Thermodynamics and Kinetics of the Electrochemical Insertion of Lithium into Tungsten Bronzes. *Solid State Ionics*, 5:351–354. doi: [10.1016/0167-2738\(81\)90265-4](https://doi.org/10.1016/0167-2738(81)90265-4)

3. Jacobsen T, West K, Atlung S (1982) Electrostatic Interactions during the Intercalation of Li in  $\text{Li}_x\text{TiS}_2$ . *Electrochim Acta* 27:1007–1011. doi: [10.1016/0013-4686\(82\)80102-3](https://doi.org/10.1016/0013-4686(82)80102-3)
4. Dahn DC, Haering RR (1982) Phase Mixtures and Staging in Intercalated  $\text{Li}_x\text{NbSe}_2$ . *Solid State Comm* 44:29–32. doi: [10.1016/0038-1098\(82\)90706-2](https://doi.org/10.1016/0038-1098(82)90706-2)
5. Green M, Kang K (1983) Sodium Tungsten Bronze Thin-Films—Variation of Chemical-Potential with Sodium Concentration. *Solid State Ionics*, 8:281–289. doi: [10.1016/0167-2738\(83\)90002-4](https://doi.org/10.1016/0167-2738(83)90002-4)
6. Raistrick ID (1983) Lithium Insertion Reactions in Tungsten and Vanadium Bronzes. *Solid State Ionics* 9:425–430. doi: [10.1016/0167-2738\(83\)90270-9](https://doi.org/10.1016/0167-2738(83)90270-9)
7. Nikolskaya EY, Tikhonov KI, Rotinyan AL (1984) Nature of the Open-Circuit Potential of  $\text{Li}^+/\text{Li}_x\text{NbSe}_2$ . *Sov Electrochem* 20:237–240
8. Tye FL (1985) Manganese-Dioxide Electrode - X. A Theoretical Treatment based on the Concept of Two Solid Solutions in the Range gamma- $\text{MnO}_2$  to delta- $\text{MnOOH}$ . *Electrochim Acta* 30:17–23. doi: [10.1016/0013-4686\(85\)80053-0](https://doi.org/10.1016/0013-4686(85)80053-0)
9. Shustova SI, Ravdel BA, Tikhonov KI. (1985) Electrode-Reactions in the Reduction of Iron Sulfides in Propylene Carbonate. *Sov Electrochem* 21:524–527
10. Ravdel BA, Pozin MY, Tikhonov KI, Rotinyan AL (1987) Thermodynamic Properties of the Electrochemical Cell:  $\text{Li} \mid \text{LiClO}_4 \text{ (Propylene Carbonate)} \mid \text{Li}_x\text{MnO}_2$ . *Sov Electrochem* 23:1459–1464
11. Toroshchina EI, Ravdel BA, Tikhonov KI (1987) Thermodynamic Properties of the Electrochemical-Cell  $\text{Li}/\text{LiClO}_4 \text{ (Propylene Carbonate)}/\text{Li}_x\text{V}_2\text{O}_5$ . *Sov Electrochem* 23:1435–1438
12. Toroshchina EI, Ravdel BA, Tikhonov KI (1991) On the Phase-Transitions and Phase-Composition in Cathode Reduction of 2H-Niobium Diselenide. *Solid State Ionics* 48:267–269. doi: [10.1016/0167-2738\(91\)90041-9](https://doi.org/10.1016/0167-2738(91)90041-9)
13. Gavriluk VI, Plakhotnik VN (1994) Thermodynamics of Compounds of Lithium Intercalation into Vanadium Pentoxide. *Russ J Phys Chem* 68:1373–1376
14. Nikolskaya EY, Tikhonov KI, Rotinyan AL, Ravdel BA (1988) Diffusion-Coefficient of Lithium Ions as a Function of Lithium Concentration in  $\text{Li}_x\text{NbSe}_2$ . *Sov Electrochem* 24:495–498
15. Toroshchina EI, Ravdel BA, Tikhonov KI (1990) Features of the Calculation of the Kinetic-Parameters of Electrochemical Reactions on Solid Cathode Materials. 2. *Sov Electrochem* 26:611–617
16. Ravdel BA (1994) Kinetics of Lithium Nickel Cobalt Oxide Electrode Material for Lithium-ion Batteries. Proceedings of the 186th Meeting of the Electrochem Soc. Miami Beach, Florida, Oct. 9–14, 1994. Abstract #638
17. Newman J, Thomas KE (2002) Proceedings of the International Meeting on Lithium Batteries, IMLB'11, Monterey, CA, June 23–28, 2002. Abstract #346
18. Yazami R, Reyner Y, Fultz B (2002) Proceedings of the International Meeting on Lithium Batteries, IMLB'11, Monterey, CA, June 23–28, 2002. Abstract #225
19. Thomas KE, Newman J (2003) Thermal Modeling of Porous Insertion Electrodes. *J Electrochem Soc* 150:A176–A192. doi: [10.1149/1.1531194](https://doi.org/10.1149/1.1531194)
20. Fultz B, Reyner Y, Swan-Wood T, Graetz J, Rez P, Ozawa Y, Lam K, Yazami R (2004) Proceedings of the 204th Meeting of The Electrochem Soc. Orlando, Florida, Oct. 12–16, 2004. Abstract #327
21. Reyner YF, Fultz B, Yazami R (2004) Proceedings of the 204th Meeting of The Electrochem Soc. Orlando, Florida, Oct. 12–16, 2004. Abstract #1361
22. Ravdel BA, Trebukhova S, Puglia FJ (2009) Thermodynamics of Electrode Materials for Lithium-Ion Batteries. Proceedings of the 216th Meeting of the Electrochem Soc. Vienna, Austria, Oct. 4–9, 2009. Abstract #640
23. Zhang Q, Guo Q, White RE (2006) A New Kinetic Equation for Intercalation Electrodes. *J Electrochem Soc* 153:A301–A309. doi: [10.1149/1.21422874](https://doi.org/10.1149/1.21422874)
24. Bazant MZ (2013) Theory of Chemical Kinetics and Charge Transfer based on Nonequilibrium Thermodynamics. *Acc Chem Res* 46:1144–1160. doi: [10.1021/ar300145c](https://doi.org/10.1021/ar300145c)
25. International Union of Pure and Applied Chemistry; <http://www.iupac.org/>. Accessed on July 19, 2013

26. Atkins PW (1994) Physical Chemistry 5th Edition. Oxford University Press, Oxford, England
27. Lewis GN (1901) The Law of Physico-Chemical Change. Proc American Acad Arts and Sci 37:47–69
28. Bard AJ, Faulkner LR (2001) Electrochemical Methods. Fundamentals and Applications 2nd Edition. John Wiley & Sons, Inc., Hoboken, New Jersey
29. Hansen M, Anderko K (1958) Constitution of Binary Alloys. McGraw-Hill, New York
30. Nikolskaya EY, Tikhonov KI, Semenovkobzar AA, Yanaki AA, Rotinyan AL (1981) Electrochemical Reduction and Oxidation of Niobium Diselenide in propylene carbonate. J Appl Chem-USSR 54:742–745
31. Nikolskaya EY, Tikhonov KI (1981) The Effects of Solvents and Electrolytes on Electrochemical Niobium Diselenide Reduction. Sov Electrochem 17:1079–1083
32. Leden I (1964) On the Thermochemistry of Stepwise Complex Formation. Pure Appl Chem 8:171–178. doi: [10.1351/pac196408020171](https://doi.org/10.1351/pac196408020171)
33. Vinogradova-Volzhinskaya EG, Ravdel BA, Tikhonov KI, Kozhevniko PS, Oshe EK, Nadezhin YS (1988) Electrochemical Reduction of Copper(II) Oxide Films in Propylene Carbonate. Russ J Electrochem 24:630–634
34. Newman J, Thomas-Alyea KE (2004) Electrochemical Systems 3rd Edition. John Wiley & Sons, Inc., Hoboken, New Jersey
35. Bockris JO'M, Reddy AKN (1998) Modern Electrochemistry, Vol. 1: Ionics 2nd Edition. Kluwer Academic/Plenum Publishers. New York, NY
36. Ravdel BA, Sheinin DA, Tikhonov KI (1987) Criterion for a Diffusion Mechanism of Processes Attended by Ion Incorporation into a Solid Electrode. Sov Electrochem 23:652–652
37. Kuta J, Yeager E (1977) Overpotential Measurements. In: Techniques of Electrochemistry, Vol. Measurements pp. 141–292, Yeager E, Salkind AJ, eds. Wiley-Interscience, New York, NY
38. Crank J (1975) The Mathematics of Diffusion. Oxford University Press, Oxford, England
39. Lide DR, ed (2001) CRC Handbook of Chemistry and Physics 82nd Edition. CRC Press, Boca Raton
40. Dahn D.C., Haering R.R. (1982) Solid State Comm., 44:29–33
41. Glasstone S, Laidler KJ, Eyring H (1941) The Theory of Rate Processes, McGraw-Hill Book Co., Inc., New York, NY
42. Vetter K (1967) Electrochemical Kinetics, Academic Press, New York, NY
43. Nikolskaya EY, Miznenko NN, Tikhonov KI (1988) Rate of the Step of Lithium Discharge and Ionization at  $\text{Li}_x\text{NbSe}_2$  Intercalate. Sov Electrochem 24:489–494
44. Munshi MZA, Smyrl WH (1991) Insertion Reactions of Sodium in  $\text{V}_6\text{O}_{13}$  Single Crystals from a Solid Polymeric Electrolyte. Solid State Ionics 45:183–189. doi: [10.1016/0167-2738\(91\)90151-Z](https://doi.org/10.1016/0167-2738(91)90151-Z)
45. Chen L, Vanzomeran A, Schoonman J (1992) Electrochemical Insertion of Lithium into  $\text{YBa}_2\text{Cu}_3\text{O}_7$ -Y Solid State Ionics 50:55–58. doi:10.1016/0167-2738(92)90036-O
46. Ratnakumar BV, Nagasubramanian G, DiStefano S, Bankston CP (1992) Kinetics of Intercalation of Lithium into  $\text{NbSe}_3$  and  $\text{TiS}_2$  Cathodes. J Electrochem Soc 139:1513–1521
47. Ogumi Z, Inaba M (2002) Carbon Anodes. Advances in Lithium-Ion Batteries. van Schalkwijk WA, Scrosatti B, eds. Kluwer Academic/Plenum Publishers, New York, NY
48. Ravdel B, Trebukhova SA, DiCarlo JF (2006) Stability of Lithium-ion Cells Evaluated from Thermodynamic Measurements. Proceedings of the 42nd Power Sources Conference, June 12–15, 2006, Philadelphia, PA, Abstract #9.3
49. West K (1989) Intercalation Compounds: Metal Ions in Chalcogenide and Oxide Hosts. In: High Conductivity Solid Ionic Conductors: Recent Trends and Applications. T.Takahashi, ed



Lithium-ion Battery Materials and Engineering  
Current Topics and Problems from the Manufacturing  
Perspective

Gulbinska, M.K. (Ed.)

2014, IX, 205 p. 79 illus., Hardcover

ISBN: 978-1-4471-6547-7